J|A|C|S
ARTICLES
Published on Web 11/22/2003

A CASSCF/MR-CI Study toward the Understanding of Wavelength-Dependent and Geometrically Memorized Photodissociation of Formic Acid

Hong-Yuan He and Wei-Hai Fang*

Contribution from the Department of Chemistry, Beijing Normal University, Beijing 100875, P. R. China

Received May 23, 2003; E-mail: fangwh@bnu.edu.cn

Abstract: The S_0, T_1, and S_1 potential energy surfaces for the HCOOH dissociation and isomerization processes have been mapped with different ab initio methods. The wavelength-dependent mechanism for the HCOOH dissociation was elucidated through the computed potential energy surfaces and the surface crossing points. The HCOOH molecules in S_1 by excitation at 248 nm mainly decay to the ground state via the S_0 and S_1 vibronic interaction, followed by molecular eliminations in the ground state. The S_1 direct dissociation to $HCO(^2A')$ + $OH(^2\Pi)$ is the dominant pathway upon photoexcitation at 240−210 nm. Meanwhile, there is a slight probability that the system relaxes to the ground state via the S_0 and S_1 vibronic interaction at these wavelengths. After irradiation of HCOOH at 193 nm, the S_1 direct dissociation into $HCO(^2A')$ + $OH(^2\Pi)$ is energetically the most favorable pathway. In view of high IC efficiency at the S_0/S_1 conical crossing, the $S_1 \rightarrow S_0$ internal conversion via the S_0/S_1 point can occur with considerable efficiency. In addition, the S_1 isomerization probably plays a dominant role in the partially conformational memory of the HCOOH photodissociation, which has been discussed in detail.

Introduction

Formic acid (HCOOH) is an important intermediate in the oxidation of unsaturated hydrocarbons in combustion.[1] Of the organic molecules observed in the interstellar medium and upper troposphere of the earth, particular attention has been devoted to formic acid,[2] because it plays an important role in the chemistry of interstellar space and it is among the most abundant pollutants in the atmosphere.[3,4] HCOOH is a molecule of great interest to experimental and theoretical chemists, because it is the simplest of the organic acids and presents itself as an ideal model compound for spectroscopic and theoretical studies of the carboxylic acids and related organic compounds.

It was recognized very early on that the absorption spectrum[5−7] of HCOOH in the region of 260−225 nm exhibits a well-developed vibrational structure superimposed on a diffuse background that merges to a continuum at a wavelength shorter than 225 nm. The transition was characterized as $n \rightarrow \pi^*$, which corresponds to an excitation of an electron from the nonbonding orbital on the oxygen atom to the antibonding π^* orbital in the carbonyl group. The OCO bend mode has been observed, and activity in this mode arises because of the planar-to-pyramidal geometry change occurring upon photon absorption. After these early studies, rotational and infrared spectra of formic acid at both low and high resolution have been extensively investigated by Baskakov,[8−11] Tan,[12,13] Moule, and Judge.[14,15] All of the fundamentals have been assigned, and the band origin has been accurately identified as 37 413.4 cm^{-1} in the $S_0 \rightarrow S_1$ spectrum.

Several experiments have been done to elucidate thermal decomposition of formic acid in the gas phase.[16−20] Meanwhile, many theoretical studies have been published on the S_0 structures of *cis*- and *trans*-HCOOH,[21−23] the barrier to the isomerization in the ground state,[24−26] and thermal decomposition.[27−30] All of these studies agree that the most important reactions in the

(1) Gardiner, W. C., Jr. *Combustion Chemistry*; Springer-Verlag: Berlin, 1984; p 294.
(2) Kaiser, R. I. *Chem. Rev.* **2002**, *102*, 1309−1358.
(3) Khwaja, H. A. *Atmos. Environ.* **1995**, *29*, 127−139.
(4) Chapman, E. G.; Kenny, D. V.; Busness, K. M.; Thorp, J. M.; Spicer, C. W. *Geophys. Res. Lett.* **1995**, *22*, 405−408.
(5) Sugarman, B. *Proc. Phys. Soc., London* **1943**, *55*, 429−430.
(6) Calvert, J. G.; Pitts, J. N., Jr. *Photochemistry*; Wiley: New York, 1966; p 428.
(7) Ng, T. L.; Bell, S. *J. Mol. Spectrosc.* **1974**, *50*, 166−181.
(8) Baskakov, O. I.; Alanko, S.; Koivusaari, M. *J. Mol. Spectrosc.* **1999**, *198*, 40−42.
(9) Baskakov, O. I. *J. Mol. Spectrosc.* **2001**, *208*, 194−196.
(10) Baskakov, O. I.; Demaison, J. *J. Mol. Spectrosc.* **2002**, *211*, 262−272 and references therein.
(11) Winnewisser, M.; Winnewisser, B. P.; Stein, M.; Birk, M.; Wagner, G.; Winnewisser, G.; Yamada, K. M.; Belov, S. P.; Baskakov, O. I. *J. Mol. Spectrosc.* **2002**, *211*, 262−272.
(12) Tan, T. L.; Goh, K. L.; Ong, P. P.; Teo, H. H. *J. Mol. Spectrosc.* **1999**, *198*, 387−392.
(13) Tan, T. L.; Goh, K. L.; Ong, P. P.; Teo, H. H. *J. Mol. Spectrosc.* **2000**, *202*, 194−206.
(14) Beaty-Travis, L. M.; Moule, D. C.; Liu, H.; Lim, E. C.; Judge, R. H. *J. Mol. Spectrosc.* **2001**, *205*, 232−238 and references therein.
(15) Beaty-Travis, L. M.; Moule, D. C.; Lim, E. C.; Judge, R. H. *J. Chem. Phys.* **2002**, *117*, 4831−4838 and references therein.
(16) Blake, P. G.; Davies, H. H.; Jackson, G. E. *J. Chem. Soc. B* **1971**, 1923.
(17) Saito, K.; Kakumoto, T.; Kuroda, H.; Torii, S.; Imamura, A. *J. Chem. Phys.* **1984**, *80*, 4989.
(18) Samsonov, Y. N.; Petrov, A. K.; Baklanov, A. V.; Vihzin, V. V. *React. Kinet. Catal. Lett.* **1976**, *5*, 197.
(19) Corkum, R.; Willis, C.; Back, R. A. *Chem. Phys.* **1977**, *24*, 13.
(20) Evans, D. K.; McAlpine, R. D.; McClusky, F. K. *Chem. Phys.* **1978**, *32*, 81.
(21) Peterson, M. R.; Csizmadia, I. G. *J. Am. Chem. Soc.* **1979**, *101*, 1076.
(22) Wiberg, K. B.; Laidig, K. E. *J. Am. Chem. Soc.* **1987**, *109*, 5935.
(23) Chang, Y.-T.; Yamaguchi, Y.; Miller, W. H.; Schaefer, H. F., III. *J. Am. Chem. Soc.* **1987**, *109*, 7245.

ground state are molecular eliminations of HCOOH to CO + H_2O and CO_2 + H_2. The barriers to the two reactions are in the range of 68−71 kcal/mol.

Photodissociation of formic acid has been extensively investigated in the gas phase. The five dissociation channels that can occur in the HCOOH photolysis are given as follows

$$\mathrm{HCOOH} + h\nu \rightarrow \mathrm{H_2} + \mathrm{CO_2} \quad (1)$$

$$\rightarrow \mathrm{H_2O} + \mathrm{CO} \quad (2)$$

$$\rightarrow \mathrm{HCO} + \mathrm{OH} \quad (3)$$

$$\rightarrow \mathrm{H} + \mathrm{COOH} \quad (4)$$

$$\rightarrow \mathrm{HCOO} + \mathrm{H} \quad (5)$$

Early work[31−34] favored molecular eliminations (1) and (2) in the spectral region of 220−260 nm. A quantum yield of 0.7−0.8 was determined for formation of the OH product.[35−40] The S_1 direct dissociation to HCO + OH was found to be a dominant pathway for the HCOOH photolysis at ∼220 nm. In addition, a small amount of CO and CO_2 was observed by static Fourier transform infrared (FTIR) spectroscopy.[41] The OH radical was also observed[42,43] from the photodissociation of HCOOH at several wavelengths between 250 and 220 nm.

The vibrationally excited products were detected using a time-resolved FTIR spectrometer[44] after laser photolysis at 248 and 193 nm. It was found that the HCOOH photodissociation at 248 nm takes place on the S_0 surface after internal conversion; meanwhile, channel (3) that produces HCO + OH radicals along the S_1 pathway has been identified upon photolysis at 193 nm. Photoinduced decomposition of HCOOH has been investigated in low-temperature rare gas matrixes, and conformational memory was observed in photodissociation of formic acid at 193 nm.[45,46] In UV photolysis of *trans*-HCOOH in solid Ar, the H_2O + CO channel dominates the H_2 + CO_2 channel, while photolysis of *cis*-HCOOH in solid Ar at 193 nm is dominated by the H_2 + CO_2 channel. The 212.8-nm photodissociation dynamics of HCOOH was investigated utilizing degenerate four-wave mixing (DFWM) spectroscopy.[47] Vacuum-UV (VUV) photodissociation of gaseous HCOOH has been studied in the 6−23 eV range using photofragment fluorescence spectroscopy and synchrotron radiation excitation.[48] The neutral and ionic dissociation processes were identified in the above study. The relaxation of the high-energy cis conformer of HCOOH to the lower-energy trans form by the tunneling mechanism has been investigated in low-temperature rare gas matrixes.[49]

As stated above, the HCOOH photodissociation has been a subject of numerous experimental studies. Yet different products were observed in these studies, and the underlying mechanism is largely unknown. As far as we know, there are only two theoretical studies[44,45] on the excited-state potential energy profiles of HCOOH up to date which are qualitatively reliable. In the present work, we report an extensive ab initio calculation carried out by employing several advanced techniques. The ground- and excited-state potential energy surfaces for HCOOH dissociations to HCO + OH, COOH + H, and HCOO + H are determined at different levels of theory. These calculated potential energy surfaces and the computed intersections between the surfaces are used to determine the most probable mechanisms leading to different photoproducts. We believe that the results reported here provide new insights into the wavelength-dependent and geometrically memorized photodissociation of formic acid.

Computational Details

Electronic states considered here in addition to the ground state were the first excited valence singlet and triplet states, $^1n\pi^*(S_1)$ and $^3n\pi^*(T_1)$. Geometries were obtained by a full optimization at the complete active space self-consistent field (CASSCF) level for each stationary structure in each given electronic state, because the CASSCF wave function has sufficient flexibility to model the large changes in electronic structure that can take place during the chemical reactions.[50] However, the complete active space formalism contains a certain amount of ambiguity in terms of which particular electrons and orbitals are chosen for inclusion. For this reason, selection of the active space becomes a crucial step of the CASSCF calculations. After preliminary calculations with a small active space that comprises eight electrons in seven orbitals, all stationary structures were further optimized at the CASSCF level with an active space comprising 18 electrons (all valence electrons for HCOOH) in 13 orbitals, hereafter referred to as CAS-(18,13). In addition to nine occupied orbitals, the C−O π^*, C−H, O−H, and C−C σ^* orbitals are used as the active orbitals. It should be pointed out that the three σ^* orbitals in the active space are actually delocalized into the whole molecular backbone with remarkable antibonding character in the C−H, O−H, and C−C regions. The cc-pVTZ basis set[51] was mainly employed in the present calculations. With use of the CAS(18,13)/cc-pVTZ structures and wave functions as the initial guess, all of the stationary structures are reoptimized at the CAS(10,8) level. Once convergence was reached, the harmonic frequencies were examined to confirm the optimized structure to be a true minimum or

(24) Fausto, R.; Batistade de Carvallo, L. A. E.; Teixeria-Dias, J. J. C.; Ramos, M. N. *J. Chem. Soc., Faraday Trans. 2* **1989**, *85*, 1945.
(25) Feller, D.; Bordon, W. T.; Davidson, E. R. *J. Comput. Chem*. **1980**, *1*, 158.
(26) Feller, D.; Bordon, W. T.; Davidson, E. R. *J. Chem. Phys*. **1979**, *71*, 4987.
(27) Ruelle, P.; Kesselring, U. W.; Nam-Tran, H. *J. Am. Chem. Soc*. **1986**, *108*, 371−375.
(28) Ruelle, P. *J. Am. Chem. Soc*. **1987**, *109*, 1722.
(29) Francisco, J. S. *J. Chem. Phys*. **1992**, *96*, 1167.
(30) Goddard, J. D.; Yamaguchi, Y.; Schaefer, H. F., III. *J. Chem. Phys*. **1992**, *96*, 1158−1168.
(31) Ramsperger, H. C.; Porter, C. W. *J. Am. Chem. Soc*. **1926**, *48*, 1267.
(32) Gorin, E.; Taylor, H. S. *J. Am. Chem. Soc*. **1934**, *56*, 2042.
(33) Burton, M. *J. Am. Chem. Soc*. **1936**, *58*, 1655.
(34) Gorden, R., Jr.; Ausloos, P. *J. Phys. Chem*. **1961**, *65*, 1033.
(35) Jolly, G. S.; McKenney, D. J.; Singleton, D. L.; Paraskevopoulos, G.; Bosard, A. R. *J. Phys. Chem*. **1986**, *90*, 6557.
(36) Singleton, D. L.; Paraskevopoulos, G.; Irwin, R. S.; Jolly, G. S.; McKenney, D. J. *J. Am. Chem. Soc*. **1988**, *110*, 7786.
(37) Singleton, D. L.; Paraskevopoulos, G.; Irwin, R. S. *J. Am. Chem. Soc*. **1989**, *111*, 5248.
(38) Jolly, G. S.; Singleton, D. L.; McKenney, D. J.; Paraskevopoulos, G. *J. Chem. Phys*. **1986**, *84*, 6662.
(39) Jolly, G. S.; Singleton, D. L.; Paraskevopoulos, G. *J. Phys. Chem*. **1987**, *91*, 3463.
(40) Singleton, D. L.; Paraskevopoulos, G.; Irwin, R. S. *J. Phys. Chem*. **1990**, *94*, 695−699.
(41) Irwin, R. S.; Singleton, D. L.; Paraskevopoulos, G.; Mclaren, R. *Int. J. Chem. Kinet*. **1994**, *26*, 219.
(42) Ebata, T.; Amano, T.; Ito, M. *J. Chem. Phys*. **1989**, *90*, 112.
(43) Brouard, M.; Omahony, J. *Chem. Phys. Lett*. **1988**, *149*, 45. Brouard, M.; Simons, J. P.; Wang, J. X. *Faraday Discuss. Chem. Soc*. **1991**, *91*, 63−72.
(44) Su, H.; He, Y.; Kong, F.; Fang, W.-H.; Liu, R.-Z. *J. Chem. Phys*. **2000**, *113*, 1891−1897.
(45) Lundell, J.; Rasanen, M. *J. Mol. Struct*. **1997**, *436/437*, 349−358.
(46) Khriachtchev, L.; Macoas, E.; Rasanen, M. *J. Am. Chem. Soc*. **2002**, *124*, 10994−10995.
(47) Lee, K. W.; Lee, K.-S.; Jung, K.-H.; Volpp, H.-R. *J. Chem. Phys*. **2002**, *117*, 9266−9274.
(48) Schwell, M.; Dulieu, F.; Jochims, H.-W.; Fillion, J.-H.; Lemaire, J.-L.; Baumgartel, H.; Leach, S. *J. Phys. Chem. A* **2002**, *106*, 10908−10918.
(49) Pettersson, M.; Macoas, E. M. S.; Khriachtchev, L.; Lundell, J.; Fausto, R.; Rasanen, M. *J. Chem. Phys*. **2002**, *117*, 9095−9098.
(50) Schmidt, M. W.; Gordon, M. S. *Annu. Rev. Phys. Chem*. **1998**, *49*, 233−266.
(51) Dunning, T. H., Jr. *J. Chem. Phys*. **1989**, *90*, 1007. Woon, D. E.; Dunning, T. H., Jr. *J. Chem. Phys*. **1993**, *98*, 1358. Peterson, K. A.; Woon, D. E.; Dunning, T. H., Jr. *J. Chem. Phys*. **1994**, *100*, 7410.

saddle point. Structural optimizations described here have been performed with the Gaussian 98 and 03 packages of programs.[52]

To refine the relative energies of the stationary structures, the single-point energy is calculated with the internally contracted MR-CI method that includes all single and double excitations relative to the CASSCF reference wave functions. A total of 18 valence electrons and all virtual orbitals are include in the MR-CI correlation calculations, with the C and O 1s electrons treated as a frozen core. The MOLPRO program package[53] was used to perform the MR-CI single-point energy calculations.

Results and Discussion

A. Equilibrium Geometries. Equilibrium geometry and electronic structure are basic, but very important, properties of a molecule. However, there is a general lack of information on the structural nature of HCOOH in excited states. Formic acid in S_0 has a planar structure and exists as trans and cis isomers with respect to the C−O single bond. They are respectively labeled by *trans*-HCOOH(S_0) and *cis*-HCOOH(S_0). The *trans*-HCOOH(S_0) structure is shown in Figure 1 along with the atomic numbers and the CAS(18,13) bond parameters. Both experiment and theory agree that the *trans*-HCOOH(S_0) is more stable with the relative energy of 4−5 kcal/mol for *cis*-HCOOH(S_0).[11,30,44] The barrier to the trans−cis isomerization was predicted to be in the range of 13 kcal/mol.[30,44] It is evident that a partial double bonding across the central O4−C2 bond has the effect of impeding the free internal rotation of the OH group.

As for the S_0 minimum species, the S_1 structure was first optimized with the C_s symmetry constraint at the CAS(10,8)/cc-pVTZ level. The obtained *cis*- and *trans*-HCOOH structures were confirmed to be the second-order saddle points on the S_1 surface by normal-mode analyses. The two imaginary frequencies (1015.5i and 259.3i cm^{-1}) correspond to the C−H wagging and the O−H torsional motions, respectively. Following the directions of the vibrational motions corresponding to the two imaginary frequencies, two nonplanar S_1 structures were found and confirmed to be minima by the CAS(10,8)/cc-pVTZ frequency calculations. The two nonplanar S_1 minimum-energy structures are referred to as *cis*-HCOOH(S_1) and *trans*-HCOOH(S_1), respectively, hereafter.

The optimized *cis*-HCOOH(S_1) and *trans*-HCOOH(S_1) structures were shown in Figure 1 along with the CAS(18,13)/cc-pVTZ bond parameters. The C2−O1 and O4−C2 bond distances are, respectively, 1.389 and 1.385 Å in the *trans*-HCOOH(S_1) equilibrium geometry, which are 0.188 and 0.057 Å longer than the corresponding values in the S_0 equilibrium structure. The O−C−O angle is decreased from 125.1° in *trans*-HCOOH(S_0) to 111.4° in *trans*-HCOOH(S_1). From the band contour analysis of the 2593 Å band,[7] the C2−O1 bond length and the O−C−O angle were derived to be, respectively, 1.407 Å and 114.4° for HCOOH in the S_1 state. The experimentally derived bond length and angle are close to the CAS(18,13)/cc-pVTZ calculated values. The lengthening of the C2−O1 bond exhibits the nature of the $n \rightarrow p^*$ transition, where the carbonyl group attempts to reduce its π-bonding character upon excitation to the S_1 state. As pointed out before, the conjugation interaction exists between the C=O π electrons and the lone pair of the OH group in the ground state. However, this interaction disappears due to the nonplanar S_1 structure. This is the reason the O4−C2 bond distance is significantly increased from S_0 to S_1.

Formic acid in the ground state has a planar structure due to the sp^2 hybridization of the C atom. The $n \rightarrow p^*$ excitation results in a rehybridization of the C atom from sp^2 to sp^3. As a consequence, the O4−C2−O1−H3 moiety in S_1 becomes pyramidal in structure. These are mainly responsible for a large change in the dihedral angle from S_0 to S_1. The dihedral angles of O4−C2−O1−H3 and H5−O4−C2−O1 are, respectively, 129.3° and 54.1° in *trans*-HCOOH(S_1), which is quite different from the corresponding values in the S_0 equilibrium geometries. The fitted S_1 potential energy surface (PES) revealed a pair of stable conformers[15] with minima at α(O4−C2−O1−H3) = 122.5°, θ(H5−O4−C2−O1) = 68.1°, and α = 135.2°, θ = 131.5°. The experimentally inferred O−H torsional (θ) and C−H wagging (α) angles for the *trans*-HCOOH(S_1) structure were close to those from the CAS(18,13)/cc-pVTZ optimizations.

As shown in Figure 1, most of the bond parameters for the T_1 structure are close to those for the corresponding S_1 geometry, because the T_1 state also originates from the $n \rightarrow p^*$ transition. However, some differences exist between the S_1 and T_1 structures. For example, the O1−C2 bond length is 0.013 Å shorter in *trans*-HCOOH(T_1) than that in *trans*-HCOOH(S_1) and the O−H torsional angle in *cis*-HCOOH(T_1) is 137.8°, that is much smaller than 176.9° in *cis*-HCOOH(S_1). Because the HCOOH molecule in S_1 has a C_1 symmetry structure, the S_1 state is mainly of the $^1n\pi^*$ character, but with a little contribution from the $\pi \rightarrow p^*$ transition. This is probably the reason the S_1 state is to some extent different from the T_1 state in the structure.

B. Cis−Trans Isomerization in the S_1 and T_1 States. The five stationary structures were found in the S_1 Franck−Condon (FC) region. As shown in Figure 2, the planar *cis*- and *trans*-HCOOH(S_1) structures are the second-order saddle points. The nonplanar *trans*-HCOOH(S_1) minimum is 2.5 kcal/mol more stable than the nonplanar *cis*-HCOOH(S_1) minimum, and the two S_1 minima are separated by a first-order saddle point labeled by TS0(S_1). With respect to the *trans*-HCOOH(S_1) minimum, the barrier to the O−H torsional motion is predicted to be 2.9 kcal/mol by the CAS(18,13)/cc-pVTZ calculations. The *cis*-HCOOH(S_1) minimum was experimentally inferred to be 1207 cm^{-1} (3.4 kcal/mol) less stable and to be separated by a torsional saddle point of 1270 cm^{-1} (3.6 kcal/mol) from the *trans*-HCOOH(S_1) equilibrium geometry.[15] In comparison with the experimental findings, the O−H torsional motion in the S_1 surface is well described by the present CAS(18,13)/cc-pVTZ calculations.

Like the S_1 state, five stationary structures were found in the FC region of the T_1 state: two planar second-order saddle points, two nonplanar minima, and one first-order saddle point that

(52) Frisch, M. J.; Trucks, G. W.; Schlegel, H. B.; Scuseria, G. E.; Robb, M. A.; Cheeseman, J. R.; Zakrzewski, V. G.; Montgomery, J. A.; Stratmann, R. E.; Burant, J. C.; Dapprich, S.; Millam, J. M.; Daniels, A. D.; Kudin, K. N.; Strain, M. C.; Farkas, O.; Tomasi, J.; Barone, V.; Cossi, M.; Cammi, R.; Mennucci, B.; Promelli, C.; Adamo, C.; Clifford, S.; Ochterski, J.; Petersson, G. A.; Ayala, P. Y.; Cui, Q.; Morokuma, K.; Malick, D. K.; Rabuck, A. D.; Raghavachari, K.; Foresman, J. B.; Cioslowski, J.; Ortiz, J. V.; Stefanov, B. B.; Liu, G.; Liashenko, A.; Piskorz, P.; Komaromi, I.; Gomperts, R.; Martin, R. L.; Fox, D. J.; Keith, T.; Al-Laham, M. A.; Peng, C. Y.; Nanayakkara, A.; Gonzalez, C.; Challacombe, M.; Gill, P. M. W.; Johnson, B. G.; Chen, W.; Wong, M. W.; Andres, J. L.; Head-Gordon, M.; Replogle, E. S.; Pople, J. A. *Gaussian 98*, revision A.3; Gaussian, Inc.: Pittsburgh, PA, 1998.

(53) MOLPRO is a package of ab initio programs written by Werner, H.-J. and Knowles, P. J. with contributions from Almlof, J.; Amos, R. D.; Cooper, D. L.; Deegan, M. J. O.; Dobbyn, A. J.; Eclert, E.; Elbert, S. T.; Hampel, C.; Lindh, R.; Lloyd, A. W.; Meyer, W.; Nicklass, A.; Peterson, K.; Pitzer, R.; Stone, A. J.; Taylor, P. R.; Mura, M. E.; Pulay, P.; Schutz, M.; Stoll, H.; Thorsteinsson, T.

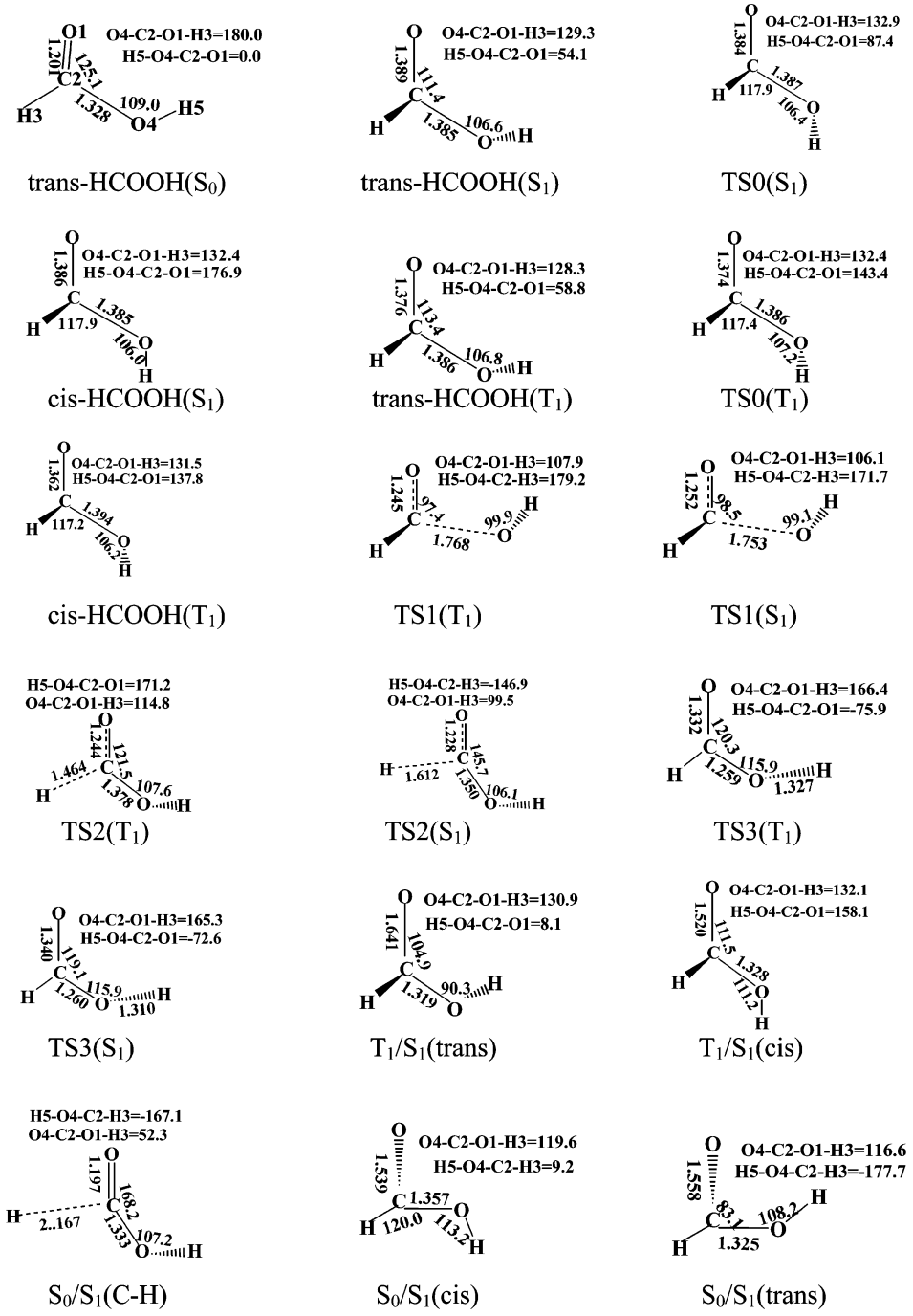

Figure 1. Schematic structures of the stationary and intersection points on different electronic states, along with the selected CAS(18,13)/cc-pVTZ bond parameters for the stationary structures and the CAS(10,8)/cc-pVTZ bond parameters for intersection structures (bond lengths in Å and bond angles in deg).

separates the two T_1 minima. The energy difference between the planar and nonplanar *trans*-HCOOH(T_1) structures is predicted to be 8.4 kcal/mol by the CAS(18,13)/cc-pVTZ calculations with the CAS(10,8)/cc-pVTZ zero-point energy corrections. The *cis*-HCOOH(T_1) minimum is 2.1 kcal/mol less stable than the *trans*-HCOOH(T_1) minimum with a barrier of 3.0 kcal/mol to the isomerization from *trans*- to *cis*-HCOOH-(T_1) at the CAS(18,13)/cc-pVTZ level.

C. The Dissociation of HCOOH into HCO + OH. The OH radical in the ground state is of $^2\Pi$ symmetry that is two-fold degenerate, and the HCO radical has a $^2A'$ ground state. When the two ground-state radicals approach each other in C_1 symmetry, they can correlate with two singlet (S_0 and S_1) and two triplet (T_1 and T_2) electronic states of HCOOH. No transition state was found on the S_0 pathway of the *trans*-HCOOH(S_0) dissociation into HCO($^2A'$) + OH($^2\Pi$). On the basis of thermochemical data,[54,55] the dissociation process was estimated to be endothermic by about 110 kcal/mol,[30,48] which is higher than the heat of formation (96.8 kcal/mol) cited in the previous work.[44] The best estimation by the present MR-CI calculations is 103 kcal/mol for the endothermic character of the *trans*-HCOOH(S_0) dissociation into HCO($^2A'$) + OH($^2\Pi$).

(54) Chase, M. W.; Davies, C. A.; Downey, J. R.; Frurip, D. J.; McDonald, R. A.; Syverud, A. N. *JANAF Thermochemical Tables*; American Institute of Physics: New York, 1986.
(55) Benson, S. W. *Thermochemical Kinetics*, 2nd ed.; Wiley: New York, 1976.

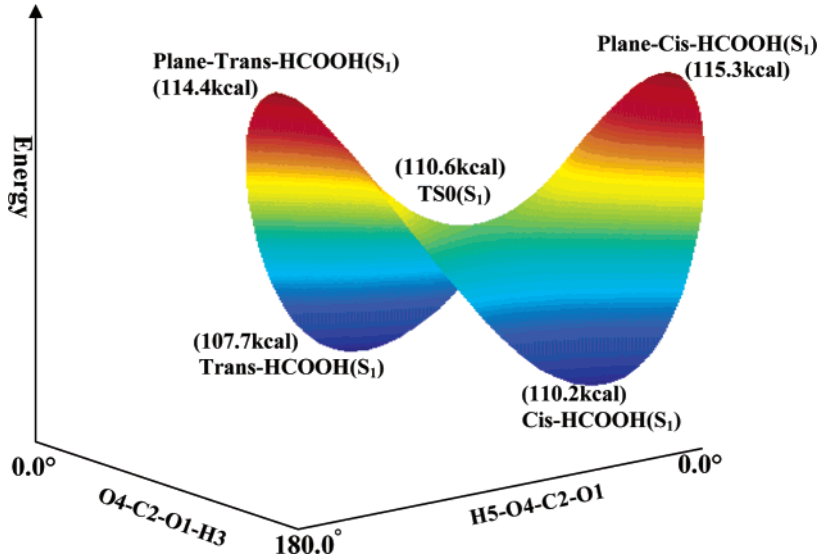

Figure 2. Schematic potential energy surface for the S_1 isomerization of HCOOH, along with energies (kcal/mol) relative to the *trans*-HCOOH(S_0) zero-level.

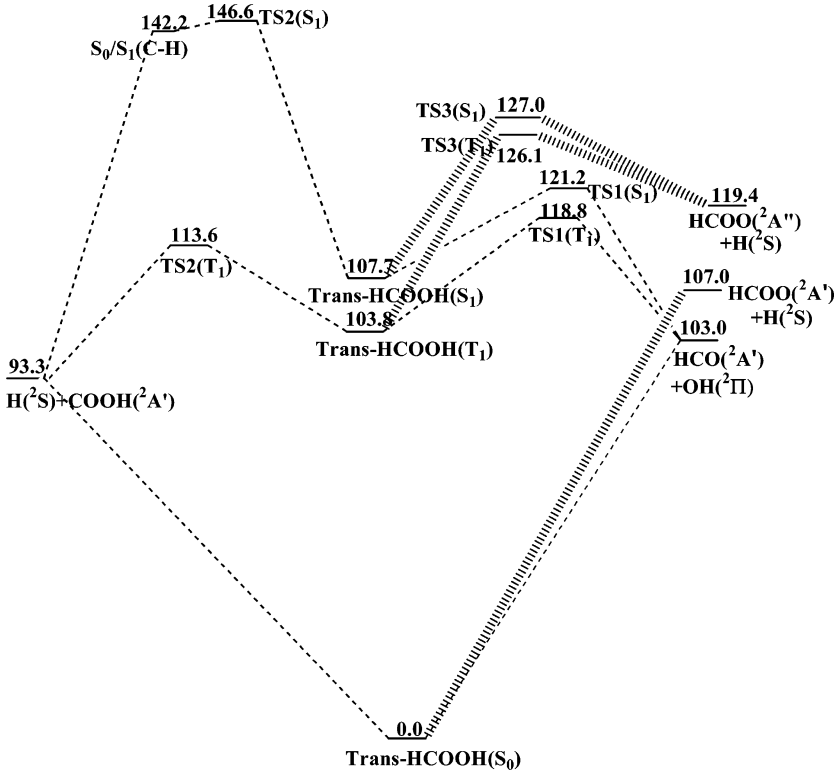

Figure 3. Schematic S_0, T_1, and S_1 potential energy surfaces for the HCOOH dissociations to HCO + OH, H + COOH, and HCOO + H, along with the MR-CI relative energies (kcal/mol).

The conjugation interaction between the lone pair of the O4 atom and C2−O1 π electrons disappears upon one-electron excitation from S_0 to S_1 or T_1. As a result of this, the dissociation of HCOOH into HCO + OH proceeds more easily along the T_1 or S_1 pathway with respect to the S_0 pathway. Unlike the S_0 dissociation, there is a barrier on the S_1 pathway for *trans*-HCOOH(S_1) dissociation into HCO($^2A'$) + OH($^2\Pi$) with the transition state labeled by TS1(S_1). The barrier height was predicted to be 13.0, 14.7, and 13.5 kcal/mol, respectively, by the CAS(10,8)/cc-pVTZ, CAS(18,13)/cc-pVTZ, and MR-CI calculations with the CAS(10,8)/cc-pVTZ zero-point energy corrections. The potential energy surfaces of the *trans*-HCOOH(S_1) dissociation into HCO($^2A'$) + OH($^2\Pi$) are shown in Figure 3 along with the MR-CI calculated relative energies. It was recognized that the $S_0 \rightarrow S_1$ electronic spectrum of HCOOH possesses a rich vibrational structure in the 268−250 nm near the UV region[14,15] that becomes diffuse at higher energies and eventually merged into a continuum at wavelength shorter than 225 nm.[7] The well-developed vibrational structure in the $S_0 \rightarrow S_1$ electronic spectrum reveals that a considerable barrier exists on the S_1 dissociation pathway. The spectrum becomes diffuse at ~250 nm and continuum at ~225 nm, which shows that the barrier to the S_1 dissociation is in the range of 7.5−20.0 kcal/mol. It is evident that the calculated barrier of

about 13.5 kcal/mol is reasonable, as compared with the experimental findings.

Like the S_1 dissociation, a transition state, labeled by TS1(T_1) hereafter, was found on the lowest triplet pathway. As shown in Figure 1, the C2−O4 distance in TS1(T_1) is 1.768 Å at the CAS(18,13)/cc-pVTZ level, which is close to that of 1.753 Å in TS1(S_1). Actually, TS1(T_1) is similar to TS1(S_1) in structure with the largest difference of 0.013 Å in bond distance and 2° in bond angle. The barrier to the T_1 dissociation of *trans*-HCOOH(T_1) into HCO(^{2}A′) + OH($^2\Pi$) was predicted to be 14.4, 15.4, and 14.9 kcal/mol, respectively, by the CAS(10,8)/cc-pVTZ, CAS(18,13)/cc-pVTZ, and UMP2/aug-cc-pVTZ calculations with the CAS(10,8)/cc-pVTZ zero-point energy correction. On the basis of the CAS(18,13)/cc-pVTZ optimized structures, the MR-CI single point calculations give the barrier of 15.0 kcal/mol. The calculations at the CASSCF, UMP2, and MR-CI levels of theory agree in predicting the barrier height of about 15 kcal/mol for the T_1 dissociation, which gives us reason to expect that dynamic electron correlation has little influence on the T_1 barrier height. A similar situation was found for the S_1 dissociation, as discussed above.

D. The Dissociation of HCOOH into H + COOH. The COOH radical in the ground state is planar with ^{2}A′ symmetry. When the ground-state radical approaches the H atom in C_1 symmetry, they can correlate with the S_0 and T_1 electronic states of HCOOH. No barrier was found above the endothermic character for the *trans*-HCOOH(S_0) dissociation into COOH(^{2}A′) + H(^{2}S) along the S_0 pathway. Previous workers[17,30,48] have cited the reaction energy of 93−96 kcal/mol for the dissociation process, which is close to the heat of formation[44] of 91.1 kcal/mol at 0° K. The energy of the separated H and COOH fragments was determined from a supermolecule calculation that puts both fragments at a large separation. This calculation was performed with the same basis set and active space as the calculation of the bound fragments. In this way, the reaction energy was calculated to be 93.3 kcal/mol for the *trans*-HCOOH(S_0) dissociation into COOH(^{2}A′) + H(^{2}S) at the MR-CI level.

The T_1 cleavage of the C−H bond can lead to formation of the H + COOH fragments in the ground state. A transition state was optimized and confirmed to be the first-order saddle point on the T_1 surface, which is referred to as TS2(T_1) hereafter. In the TS2(T_1) structure depicted in Figure 1, the COOH moiety is nearly coplanar, while the H atom lies above of the COOH plane with the C−H distance of 1.464 Å at the CAS(18,13)/cc-pVTZ level. The potential barrier for the C−H bond fission along the T_1 pathway was predicted to be 16.2 kcal/mol by the CAS(18,13)/cc-pVTZ calculations. On the CAS(18,13)/cc-pVTZ optimized structures of HCOOH(T_1) and TS2(T_1), the MR-CI single-point energy calculations give the barrier of 9.8 kcal/mol, as shown in Figure 3. The TS2(T_1) structure is also optimized at the UMP2/aug-cc-pVTZ level, which predicts the barrier to be 12.1 kcal/mol for the T_1 dissociation of HCOOH to COOH(^{2}A′) + H(^{2}S).

Qualitatively, the HCOOH molecules in the S_1 state correlate with an excited electronic state of the COOH + H fragments. The optimized transition state of TS2(S_1) on the S_1 pathway was shown in Figure 1 along with CAS(18,13)/cc-pVTZ bond parameters. The first observation is that TS2(S_1) is quite different from TS2(T_1) in structure. The C−H distance in TS2(S_1) is 1.612 Å, which is 0.148 Å longer than that in TS2(T_1). The O−C−O angle is increased from 121.5° in TS2(T_1) to 145.7° in TS2(S_1). In TS2(T_1), the COOH moiety is almost coplanar and the departure H3 atom lies above the COOH plane, while the H3 atom departs with the H5−O4−C2−H3 dihedral angle of about 150° in TS2(S_1). Several ab initio studies[56,57] have been conducted on the COOH radical. The radical in the ground state is planar with ^{2}A′ symmetry, and the O−C−O angle is about 120°. This angle was predicted to be 174.4° in the first excited state (^{2}A″) of the radical by the CCSD(T)/cc-pVTZ calculations.[57] The O−C−O angle in TS2(S_1) is closer to that in the ^{2}A″ excited state of the COOH radical, while the C2−O1 bond length of 1.228 Å in TS2(S_1) is closer to that of 1.183 Å in the ^{2}A′ ground state of the radical.

The IRC calculations have been carried out at the CAS(10,8)/cc-pVTZ level with the TS2(S_1) structure as the starting point. On the reactant side, TS2(S_1) was confirmed to connect the *trans*-HCOOH(S_1). However, on the product side, the problem of convergence was encountered during the state-specific CASSCF optimization of the IRC pathway. The S_0 and S_1 surfaces approach each other at the large C−H separate, which results in the breakdown of the Born−Oppenheimer approximation. This implies that we have to consider the S_1 and S_0 surface intersection. The geometry optimization for the intersection was carried out with the state-averaged CAS(10,8)/cc-pVTZ method by searching for the lowest energy point of the surface crossing seam starting from the last successful point of the product-side IRC pathway on the S_1 surface. The S_1 and S_0 surface intersection, referred to as S_1/S_0(C−H) in Figure 1, was found at the C2−H3 distance of 2.167 Å. The mechanism of the S_1 C−H bond cleavage can be represented as HCOOH(S_1) → TS2(S_1) → S_1/S_0(C−H) → COOH(^{2}A′) + H (^{2}S). It is also possible that the hot parent HCOOH(S_0) molecule can be formed after funneling through the S_1/S_0(C−H) conical intersection. The potential energy surface of the *trans*-HCOOH(S_1) dissociation to H(^{2}S) and COOH(^{2}A′) is shown in Figure 3 along with the MR-CI relative energies. The relatively high barrier to the C−H bond cleavage on the S_1 surface originates from the highly excited energy from ^{2}A′ to ^{2}A″ for the COOH radical. The CCSD(T)/cc-pVTZ calculations predict that the ^{2}A″ state of COOH has an energy of 70.7 kcal/mol[57] above the zero level of its ^{2}A′ ground state.

E. The Dissociation of HCOOH into HCOO + H. As shown in Figure 3, the mechanism of the HCOOH dissociation to HCOO + H is different from that for the dissociation to HCO + OH or H + COOH. Two transition states were optimized and confirmed to be the first-order saddle points on the S_1 and T_1 pathways to HCOO + H, which are respectively denoted by TS3(S_1) and TS3(T_1). A comparison of the TS3(S_1) and TS3(T_1) bond parameters in Figure 1 reveals that the two transition states have similar structures, which predicts that TS3(S_1) and TS3(T_1) lead to the fragments in the same electronic state. The state-averaged CAS(10,8)/cc-pVTZ optimizations have been performed with use of the TS3(S_1) and TS3(T_1) structures as the initial guesses. The S_1 and T_1 surface crossing was not found until the dissociation limit. This gives further evidence that the T_1 and S_1 O−H cleavages yield the same fragments of HCOO(^{2}A″) + H(^{2}S).

(56) Duncan, T. V.; Miller, C. E. *J. Chem. Phys.* **2000**, *113*, 5138−5140 and references therein.
(57) Li, Y.; Francisco, J. S. *J. Chem. Phys.* **2000**, *113*, 7963−7970.

As shown in Figure 3, the dissociation along the S_0 pathway is endothermic by 107 kcal/mol with no barrier above the endothermicity. The thermochemical threshold energy for the HCOOH(S_0) dissociation into HCOO + H was cited to be 106−111 kcal/mol in refs 30, 44, and 48. The barrier height on the T_1 pathway is calculated to be 27.5, 23.8, and 22.3 kcal/mol at the CAS(10,8), CAS(18,13), and MR-CI levels of theory with the CAS(10,8)/cc-pVTZ zero-point energy correction. The corresponding barrier becomes 23.0, 20.3, and 19.3 kcal/mol for the S_1 dissociation to HCOO(^{2}A″) and H(^{2}S). The small difference in the T_1 and S_1 barrier heights supports the above conclusion that the O−H bond cleavages along the T_1 and S_1 pathways yield the fragments in the same electronic state. In comparison with the S_1 C−H bond fission, the O−H bond cleavage has a lower barrier on the S_1 pathway. This mainly originates from the small energy difference between the ^{2}A′ ground state and the ^{2}A″ excited state for the HCOO radical. There exist numerous theoretical studies on the HCOO radical, which has been reviewed by Roos and co-workers.[58] The ^{2}A″ state of the HCOO radical is 14.1 kcal/mol above the $^2A_1$ ground state at the CASPT2 level. The relative energy of the ^{2}A″ state was experimentally estimated at T_0 = 0.536 eV (12.4 kcal/mol).[59]

Before ending this subsection, we comment briefly on the accuracy of the calculated energies in the present work. The adiabatic excitation energy from *trans*-HCOOH(S_0) to *trans*-HCOOH(S_1) was predicted be 113.0, 110.3, and 107.7 kcal/mol, respectively, by the CAS(10,8)/cc-pVTZ, CAS(18,13)/cc-pVTZ, and MR-CI calculations, which is very close to the band origin of 37 413.4 cm^{-1} (107.0 kcal/mol) in the $S_0 \rightarrow S_1$ spectrum of HCOOH.[15] Relative to *trans*-HCOOH(S_1), the *cis*-HCOOH(S_1) isomer has an energy of 2.5 kcal/mol with the barrier of 2.9 kcal/mol for the trans−cis isomerization. The relative energy of *cis*-HCOOH(S_1) was experimentally inferred to be 1207 cm^{-1} (3.4 kcal/mol), and the barrier to the trans−cis isomerization was estimated to be 1270 cm^{-1} (3.6 kcal/mol)[15] above the *trans*-HCOOH(S_1) isomer. As far as we know, the barriers to the S_1 and T_1 dissociations of HCOOH have not been determined experimentally. Yet the CH_3COOH dissociation into CH_3CO + OH along the S_1 pathway was found to have a barrier of 13−15 kcal/mol from the previous experimental and theoretical studies,[60−63] which is very close the present calculated value of 13.0−14.0 kcal/mol for the *trans*-HCOOH(S_1) dissociation into HCO + OH. On the CAS(18,13)/cc-pVTZ optimized structures, the MR-CI calculated dissociation energies are close to the corresponding heats of formation at 0 K, as discussed before. From the above comparison, we believe that the present calculations give a balanced representation of the HCOOH dissociations along the S_0, S_1, and T_1 pathways, the surface topology obtained in this work should be reliable, and the detailed energies are in error by a few kcal/mol.

F. Surface Intersections and Mechanistic Aspects. The S_0 and S_1 surface crossing (S_0/S_1) near the FC geometry was determined by the state-averaged CAS(10,8)/cc-pVTZ optimizations[64] without any symmetry constraints. The resulting S_0/S_1(cis) and S_0/S_1(trans) structures are shown in Figure 1. In comparison with the corresponding S_1 or S_0 minimum, the largest change is associated with the C2−O1 distance. The derivative coupling and gradient difference vectors at the S_0/S_1(trans) structure are plotted in Figure 4. The derivative coupling vectors mainly correspond to the C2−O1 and C2−O4 stretching, and the O4−C2−O1 bending motions, which could lead to the system in the S_1 minimum. However, the gradient difference vectors correspond to a significant decrease of the C2−O1 distance and a remarkable increase of the O4−C2−O1 angle, resulting in the HCOOH molecule in the S_0 state. When Slater determinants in the state-averaged CAS(10,8)/cc-pVTZ calculations were used,[65,66] two intersection points between the T_1 and S_1 surfaces in the FC region were determined, labeled by T_1/S_1(cis) and T_1/S_1(trans) hereafter. In comparison with the corresponding S_1 minima, the C2−O1 distance is significantly lengthened, while the C2−O4 bond is considerably shortened in the T_1/S_1(cis) and T_1/S_1(trans) structures, especially for the T_1/S_1(trans) structure.

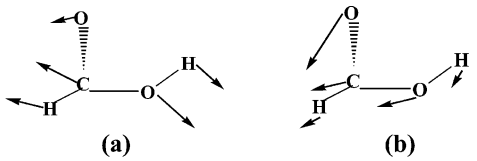

Figure 4. The schematic derivative coupling vectors (a) and gradient difference vectors (b) at the S_0/S_1(trans) structure.

Upon photoexcitation of HCOOH at 260−248 nm that corresponds to the excitation energy of 110−115 kcal/mol, the S_1 direct dissociations, ISC via the T_1/S_1 point and IC through the S_0/S_1 point, are all inaccessible in energy. In this case, the system relaxes mainly to the ground state via the S_0 and S_1 vibronic interaction, besides radiation processes. As pointed out before, the $n \rightarrow \pi^*$ excitation leads to the pyramidal S_1 equilibrium geometry. The normal modes are not only displaced and distorted but also mixed with each other after the $n \rightarrow \pi^*$ electronic excitation. The CAS(10,8)/cc-pVTZ frequency calculations reveal that there is a large change in the S_1 vibrational frequencies and heavy mixing of the C1−O2 stretching and the H3−C2−O1 and O1−C2−O4 bending modes with respect to the ground-state normal modes and frequencies. The frequency change and mode mixing make the $S_1 \rightarrow S_0$ internal conversion occur with considerable efficiency, by increasing the vibrational part of the IC rate constant.[67]

After relaxation to the S_0 state, the system is left with sufficient internal energies to overcome the barriers on the S_0 pathways, leading to formation of $CO_2 + H_2$ and $CO + H_2O$. The dissociation channels (3), (4), and (5) are highly endothermic along the S_0 pathways, and they are not in competition with the molecular eliminations (1) and (2) in the ground state. Therefore, IC to S_0 followed by the molecular eliminations is the dominant pathway for the HCOOH photodissociation at 248 nm and longer wavelength. A large amount of the vibrationally

(58) Rauk, A.; Yu, D.; Borowski, P.; Roos, B. *Chem. Phys.* **1995**, *197*, 73−80.
(59) Kim, E. H.; Bradforth, S. E.; Arnold, D. W.; Metz, R. B.; Neumark, D. M. *J. Chem. Phys.* **1995**, *103*, 7801−7814.
(60) Hunnicutt, S. S.; Waits, L. D.; Guest, J. A. *J. Phys. Chem.* **1989**, *93*, 5188.
(61) Hunnicutt, S. S.; Waits, L. D.; Guest, J. A. *J. Phys. Chem.* **1991**, *95*, 562.
(62) Peterman, D. R.; Daniel, R. G.; Horwitz, R. J. Guest, J. A. *Chem. Phys. Lett.* **1995**, *236*, 564.
(63) Fang, W. H.; Liu, R. Z.; Zheng, X.; Phillips, D. L. *J. Org. Chem.* **2002**, *67*, 8407−8415.
(64) Bearpark, M. J.; Robb, M. A.; Schlegel, H. B. *Chem. Phys. Lett.* **1994**, *223*, 269.
(65) Ragazos, I. N.; Robb, M. A.; Bernardi, F.; Olivucci, M. *Chem. Phys. Lett.* **1992**, *197*, 217.
(66) Bernardi, F.; Olivucci, M.; Robb, M. A. *Chem. Soc. Rev.* **1996**, *25*, 321−328.
(67) Mebel, A. M.; Hayashi, M.; Liang, K. K.; Lin, S. H. *J. Phys. Chem. A* **1999**, *103*, 10674−10690 and references therein.

excited CO and CO_2 was observed by time-resolved FTIR spectroscopy after irradiation of HCOOH at 248 nm.[44]

The HCOOH molecules populated in S_1 by photoexcitation at 240−210 nm possess the internal energies of 120−135 kcal/mol. Under this condition, the S_1 direct dissociation to HCO(^{2}A′) + OH($^2\Pi$) and ISC via the T_1/S_1(cis) point are favorable in energy. However, the $S_1 \rightarrow T_1$ ISC is a spin-forbidden process. On the basis of the calculated spin−orbit coupling matrix element and differences of energy gradients at the T_1/S_1(cis) point, the probability factor (a transition probability per passage through the crossing seam) from S_1 to T_1 is estimated to be about 5.5×10^{-4} by the Landau−Zener law.[68] The rate of the $S_1 \rightarrow T_1$ ISC process is reduced by a factor of about 10^{-4} if the intersystem crossing is treated as a spin-allowed process. Experimentally, a nonstatistical spin−orbit state distribution for the OH radical was observed in the HCOOH photolysis,[47] which implies the absence of any interactions with nearby triplet states during the HCOOH dissociation to HCO + OH. From the above discussion, we come to the conclusion that the S_1 direct dissociation to HCO(^{2}A′) + OH($^2\Pi$) is the dominant pathway for the *trans*-HCOOH(S_1) deactivation, and the $S_1 \rightarrow T_1$ intersystem crossing is not in competition with the S_1 direct dissociation. This is the reason a high quantum yield was experimentally observed for formation of the OH product for the HCOOH photolysis at 220, 222, 225, and 212.8 nm.[35−43,47] Meanwhile, there is a little probability that the system relaxes to the ground state via the S_0 and S_1 vibronic interaction, as discussed before. This is consistent with the experimental fact that a small amount of CO and CO_2 was observed by static FTIR spectroscopy.[41]

The band origin of the $\pi \rightarrow \pi^*$ transition was experimentally assigned at 8.1 eV (~187 kcal/mol) for HCOOH.[48,69] Therefore, photoexcitation at 193 nm (~148 kcal/mol) mainly leads to the HCOOH molecules in the S_1 state, although the excitation may occur in the long wavelength tail of the $\pi \rightarrow \pi^*$ band. The S_1 direct dissociations, ISC via the T_1/S_1 point and IC through the S_0/S_1 point, are energetically accessible upon photoexcitation at 193 nm. Reaction (4) is not in competition with reaction (3), due to a high barrier on the S_1 pathway to H(^{2}S) + COOH(^{2}A′). The dissociation into COOH and H was not observed even after photoexcitation[48] of HCOOH at 13.0 eV. The initial excitation is mainly located in the C═O region, and the α C−O single bond probably cleaves before the internal energies relax to the β O−H bond. In addition, more energy is required for the S_1 O−H bond fission, as compared with the α cleavage of the C−O single bond along the S_1 pathway. Actually, the emission of HCOO formed in the VUV dissociation of HCOOH was observed at the excitation energy of 12 eV.[48] Therefore, the S_1 direct dissociation into HCO(^{2}A′) + OH($^2\Pi$) is energetically the most favorable pathway for the HCOOH photolysis in the wavelength range of 193−220 nm.

In comparison with the FC geometry in the S_1 state, the main changes in the S_0/S_1 intersection structure are associated with the C2−O1 distance and the O4−C2−O1−H3 dihedral angle. There exists a considerable force to drive the C−O stretching and the O−C−O bending motions upon vertical excitation to

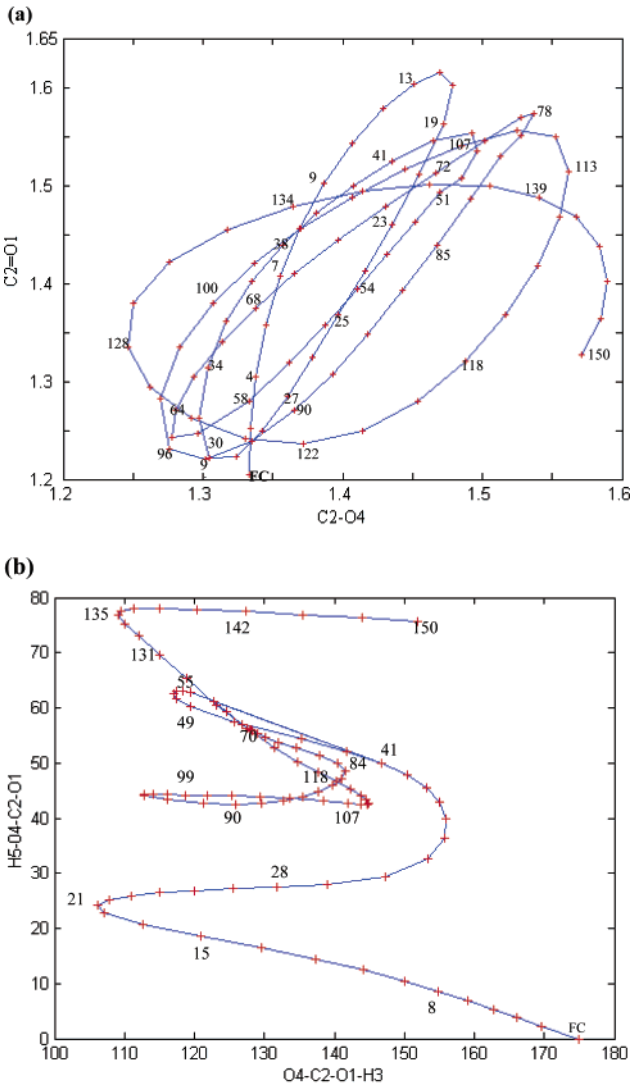

Figure 5. (a) Relaxation process from the S_1 Franck−Condon geometry of HCOOH, time dependence of the C−O distances. The labeled numbers denote time (fs). (b) Relaxation process from the S_1 Franck−Condon geometry of HCOOH, time dependence of the dihedral angles. The labeled numbers denote time (fs).

the S_1 state. The C2−O1 distance is, respectively, 1.201, 1.389, and 1.558 Å in the S_1 FC geometry, the *trans*-HCOOH(S_1) minimum, and the S_0/S_1(trans) structure. The wave packets that start from the FC geometry in S_1 can propagate to the S_0/S_1-(trans) intersection point in the process of relaxation to the *trans*-HCOOH(S_1) minimum. To give further evidence for this, we performed a classical trajectory calculation using a Born−Oppenheimer molecular dynamics model.[70] The initial conditions for trajectory calculations have been chosen to simulate the experimental photodissociation of HCOOH at 193 nm. Trajectory is started from the S_1 FC geometry with a step size of 0.3 amu$^{1/2}$ bohr. The structural relaxation processes are shown Figure 5a and b, from which it can be seen that the trajectory reaches the S_0/S_1(trans) intersection region a few times before relaxation to the S_1 minimum and the C2−O4 bond cleavage. The MR-CI calculations of global S_0 and S_1 potential energy surfaces and the time-dependent quantum wave packet study

(68) Harvey, J. N.; Aschi, M. *Phys. Chem. Chem. Phys.* **1999**, *1*, 5555−5563 and references therein.
(69) Leach, S.; Schwell, M.; Dulieu, F.; Chotin, J.-L.; Jochims, H.-W.; Baumgartel, H. *Phys. Chem. Chem. Phys.* **2002**, *4*, 5025−5039 and references therein.
(70) Li, X.; Millam, J. M.; Schlegel, S. H. *J. Chem. Phys.* **2000**, *113*, 10062−10067.

of the nonadiabatic photodissociation dynamics for HCOOH are in progress and will be reported in due course.

The S_0/S_1(trans) structure was confirmed to be a conical crossing point between the S_0 and S_1 surfaces by the state-averaged CAS(10,8)/cc-pVTZ calculations. The time scale for the $S_1 \rightarrow S_0$ IC process via the conical intersection is expected to be on the order of a vibrational period.[66] In view of high IC efficiency at the S_0/S_1(trans) structure, the internal conversion from S_1 to S_0 via the S_0/S_1(trans) point can occur with considerable efficiency upon photoexcitation of *trans*-HCOOH-(S_0) at 193 nm. Vibrationally excited CO and CO_2 were observed at 193-nm photolysis,[44] which is a result of the $S_1 \rightarrow S_0$ internal conversion followed by the molecular eliminations in the ground state. Meanwhile, the S_1 direct dissociation into $HCO(^2A') + OH(^2\Pi)$ has been identified as another important channel for the HCOOH photodissociation at 193 nm.[44]

Upon photolysis of *trans*-HCOOH at 248 and 193 nm, molecular elimination of HCOOH to $CO + H_2O$ was found to have some preference over formation of $CO_2 + H_2$. However, $CO_2 + H_2$ becomes dominant products after irradiation of *cis*-HCOOH at 193 nm.[44−46] The experimental findings clearly show that some of the HCOOH molecules are geometrically memorized in the photoinduced molecular eliminations. This has been elucidated on the basis of the stationary structures in the S_0 potential energy surface.[46] The shape of the S_1 potential energy surface is expected to play a dominant role in determining the short-lived dynamics on S_1.[71] Photoexcitation of the HCOOH molecule at 193 nm produces a replica of its S_0 equilibrium geometry on the S_1 surface. The directions of nonzero energy gradients at the S_1 FC geometry control the redistribution of the initial excitation energy among the C═O stretching, the C−H out-of-plane wagging, and the O−H torsional modes. Only following the direction of the C═O stretching vibration, structural optimizations lead to formation of the planar *cis*-HCOOH(S_1) or *trans*-HCOOH(S_1) structure (the second-order saddle point), as shown in Figure 2. Upon further release of the constraint of the C−H wagging and O−H torsional degrees of freedom, the planar *trans*-HCOOH(S_1) structure mainly relaxes to the *trans*-HCOOH(S_1) minimum, but the *cis*-HCOOH-(S_1) minimum can be produced with considerable probability, due to the nonzero O−H torsional force. As shown in Figure 5b, after 150-fs relaxation, the H5−O4−C2−O1 dihedral angle is increased from 0° in the S_1 FC geometry to ∼80° that is close to the value of 87.4° in TS0(S_1). The time scale for the S_1 trans−cis isomerization is estimated to be on the order of picoseconds. The S_1 isomerization probably plays a dominant role in the partially conformational memory of the HCOOH photodissociation.

Summary

The S_0, T_1, and S_1 potential energy surfaces for the HCOOH dissociation and isomerization processes have been mapped with different ab initio methods. The wavelength-dependent mechanisms leading to different photoproducts were determined through the computed potential energy surfaces and the surface crossing points. Irradiation of the HCOOH molecules to the S_1 state using 248-nm light does not provide enough internal energy to overcome the barriers on the S_1 pathways, and the S_0/S_1 and T_1/S_1 intersection points are energetically inaccessible at this excited wavelength. In this case, the HCOOH molecules decay mainly to the ground state via the S_0 and S_1 vibronic interaction, which is followed by the molecular eliminations to form $CO + H_2O$ and $CO_2 + H_2$. The HCOOH molecules are populated in S_1 by photoexcitation at 240−210 nm with the internal energies of 120−135 kcal/mol. The S_1 direct dissociation to $HCO(^2A') + OH(^2\Pi)$ and ISC via the T_1/S_1(cis) point is favorable in energy. However, the S_1 direct dissociation to $HCO(^2A') + OH(^2\Pi)$ is the dominant pathway for the *trans*-HCOOH(S_1) deactivation. This is the reason the predominant product channel was observed to be $HCO(^2A')$ and $OH(^2\Pi)$ for the HCOOH photolysis at ∼220 nm. Meanwhile, there is a slight probability that the system relaxes to the ground state via the S_0 and S_1 vibronic interaction upon photoexcitation at 240−210 nm. The S_1 direct dissociations, ISC via the T_1/S_1 point and IC through the S_0/S_1 point, are all accessible in energy upon photoexcitation at 193 nm. However, the S_1 direct dissociation into $HCO(^2A') + OH(^2\Pi)$ is energetically the most favorable pathway. In view of high IC efficiency at the S_0/S_1 conical crossing structure, the $S_1 \rightarrow S_0$ internal conversion via the S_0/S_1 point can occur with considerable efficiency at this excitation wavelength. In comparison with experimental findings, the present calculations provide a reasonable description of the S_1 isomerization, which probably plays a dominant role in the partially conformational memory of the HCOOH photodissociation.

Acknowledgment. This work has been supported by the National Natural Science Foundation of China (Grant Nos. 20073005 and 20233020) and by the Ministry of Science and Technology of China (Grant No. 2002CB613406).

Supporting Information Available: Structures and energies of the stationary points reported in the present work (PDF). This material is available free of charge via the Internet at http://pubs.acs.org.

JA0363157

(71) Garavelli, M.; Bernardi, F.; Olivucci, M.; Vreven, T.; Klein, S.; Celani, P.; Robb, M. A. *Faraday Discuss.* **1998**, *110*, 51−71.